Bioorganic & Medicinal Chemistry Letters xxx (2015) xxx–xxx

Contents lists available at ScienceDirect

Bioorganic & Medicinal Chemistry Letters

journal homepage: www.elsevier.com/locate/bmcl

Discovery of α-mangostin as a novel competitive inhibitor against mutant isocitrate dehydrogenase-1

Hyo-Joon Kim [a], Xiang Fei [b], Seok-Cheol Cho [c], Bu Young Choi [c], Hee-Chul Ahn [a], Kyeong Lee [a], Seung-Yong Seo [b], Young-Sam Keum [a,*]

[a] College of Pharmacy, Dongguk University, Goyang, Gyeonggi-do 410-820, Republic of Korea
[b] College of Pharmacy and Gachon Institute of Pharmaceutical Sciences, Gachon University, Incheon 406-779, Republic of Korea
[c] Department of Pharmaceutical Science and Engineering, Seowon University, Cheongju, Chungbuk 361-742, Republic of Korea

ARTICLE INFO

Article history:
Received 9 July 2015
Revised 23 September 2015
Accepted 13 October 2015
Available online xxxx

Keywords:
Isocitrate dehydrogenase-1 (IDH1)
α-Mangostin
α-Ketoglutarate (α-KG)
(*R*)-2-Hydroxyglutarate (*R*-2HG)

ABSTRACT

Somatic heterozygous mutations of isocitrate dehydrogenase-1 (IDH1) are abundantly found in several types of cancer and strongly implicate altered metabolism in carcinogenesis. In the present study, we have identified α-mangostin as a novel selective inhibitor of mutant IDH1 (IDH1-R132H). We have observed that α-mangostin competitively inhibits the binding of α-ketoglutarate (α-KG) to IDH1-R132H. The structure–relationship study reveals that α-mangostin exhibits the strongest core inhibitor structure. Finally, we have observed that α-mangostin selectively promotes demethylation of 5-methylcytosine (5mC) and histone H3 trimethylated lysine residues in IDH1 (+/R132H) MCF10A cells, presumably via restoring the activity of cellular α-KG-dependent DNA hydroxylases and histone H3 lysine demethylases. Collectively, we provide evidence that α-mangostin selectively inhibits IDH1-R132H.

A close association between metabolism and cancer has been held since the discovery by Otto Warburg that tumor cells rapidly take up glucose and convert most of it to lactate even in the presence of oxygen, a phenomenon commonly referred to as 'Warburg effect' or 'aerobic glycolysis'.[1] Although detailed molecular mechanisms of this metabolic shift in cancer are largely unknown, it provides a theoretical basis for radiolabeled fluorodeoxyglucose-positron emission tomography (^{18}FDG-PET) that is widely used for the detection of tumors in the clinic. Most notably, the genetic link between metabolism and cancer was strengthened in the last decade thanks to the identification of unexpected metabolic gene alterations in cancer by the next-generation sequencing.[2]

Malignant glioma originates from the central nervous system and is highly refractory to chemotherapy and radiotherapy. By conducting the genome-wide mutation analysis, Parsons et al. have made an observation that missense mutations in the isocitrate dehydrogenase-1 (IDH1) frequently occur in grade II–III primary gliomas and secondary glioblastomas multiforme.[3] Follow-up studies have demonstrated that analogous IDH1 mutations are also found in other types of cancers, including acute myeloid leukemia (AML), chondrosarcomas, and cholangiocarcinoma.[4] IDH1 mutations exhibit two interesting features: they are heterozygous and exclusively confined to a single amino acid residue, arginine-132, which is mostly substituted into histidine (IDH1-R132H).[5] IDH1 forms a homodimer in the cytoplasm and catalyzes the reversible oxidative decarboxylation of isocitrate (ICT) into α-ketoglutarate (α-KG) in the tricarboxylic acid cycle with a concomitant production of reduced nicotinamide adenine dinucleotide phosphate (NADPH) (Fig. 1A). In addition, mutant IDH1 is known to possess a neomorphic activity: it can irreversibly transform α-KG into a stereospecific oncometabolite, (*R*)-2-hydroxyglutarate (*R*-2HG) by utilizing NADPH as a cofactor (Fig. 1A).[6]

In the present study, we have attempted to find out a selective chemical inhibitor of IDH1-R132H. To accomplish this goal, pure recombinant IDH1 and IDH1-R132H proteins were obtained via IPTG induction in *Escherichia coli*, followed by a nickel-based affinity purification and dialysis,[7] and their activity was indirectly assessed by measuring the amount of NADPH level via spectrophotometry at 340 nm in vitro.[8] Based on this experimental setup, we evaluated the effects of 60 natural compounds derived from our in-house chemical library on recombinant IDH1 and IDH1-R132H and observed that α-mangostin exhibited a selective inhibitory effect on IDH1-R132H, but not on IDH1 (Table 1). By conducting the steady-state kinetic analysis, we observed that α-mangostin significantly increased the K_m of α-KG with K_i value around at 2.8 μM, but it did not affect the maximal velocity (V_{max}) of IDH1-R132H (Fig. 1B).[9] This result suggests that α-mangostin is a competitive

* Corresponding author. Tel.: +82 31 961 5215; fax: +82 31 961 5206.
E-mail address: keum03@dongguk.edu (Y.-S. Keum).

http://dx.doi.org/10.1016/j.bmcl.2015.10.034
0960-894X/

A

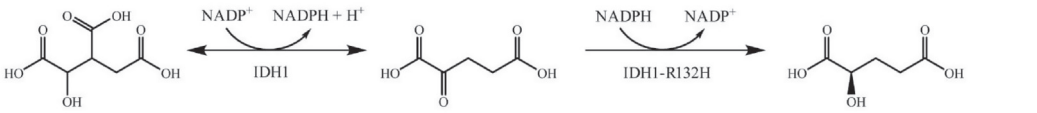

B

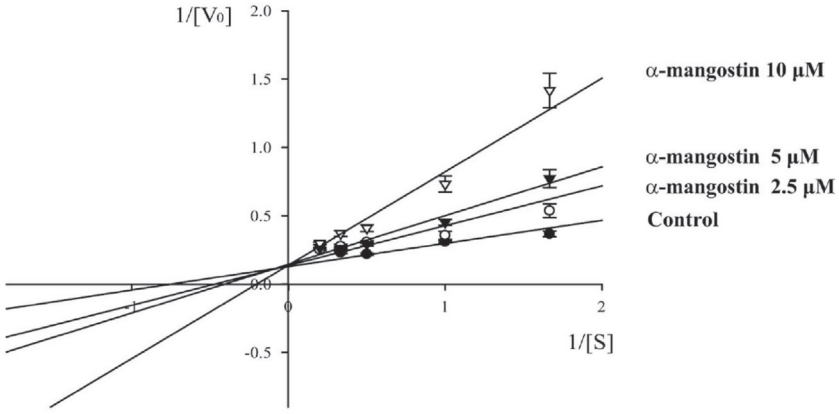

α-mangostin (μM)	NADPH (μM)	Varied Substrate	Vmax (μM/sec/mg)	Km (mM)	Ki (μM)
0	150	α-KG	7.29 ± 0.1048	1.17 ± 0.0827	2.85 ± 0.2981
2.5	150	α-KG	7.33 ± 0.1403	2.13 ± 0.0807	
5	150	α-KG	6.90 ± 0.1569	2.46 ± 0.1142	
10	150	α-KG	7.21 ± 0.3105	4.93 ± 0.3305	

Figure 1. Competitive inhibition of the IDH1-R132H activity by α-mangostin. (A) Illustration of IDH1 and IDH1-R132H metabolic reactions and (B) the acquisition of the steady-state kinetic parameters of IDH1-R132H in response to treatment of α-mangostin.

inhibitor of IDH1-R132H. We next attempted to interrogate the structure–activity relationship (SAR) of α-mangostin against IDH1-R132H. To this end, we envisioned the design of α-mangostin derivatives, in which some substituents on phenol groups on C3, C6 and C7 positions of xanthone skeleton could be varied in order to increase the binding effect on IDH1-R132H. In this regard, a series of α-mangostin derivatives have been synthesized newly or in the similar with the previous report (Scheme 1).[10] The treatment of α-mangostin (**1**) with allyl bromide and K_2CO_3 afforded both of C6-allyl and C3,6-diallyl xanthones. The diallyl xanthone was converted to the C3-allyl xanthone (**2**) by selective deallylation. The C6-allyl xanthone was treated with diethylcarbamoyl chloride and iodomethane, respectively, followed by the deallylation to afford two α-mangostin derivatives (**3** and **4**) containing *N*,*N*-diethylcarbamoyl and methyl on C-3 position. Two α-mangostin derivatives having a carbamoyl group on C6 position were prepared by using *N*,*N*-diethylcarbamoyl chloride and morpholine-4-carbonyl chloride. By the previous method, C7-modified derivatives **8** and **9** were prepared. The synthesized α-mangostin derivatives were evaluated towards IDH1-R132H. As a result, we observed that **2**, **3**, **6**, **7**, and **9** failed to exhibit inhibitory activities on IDH1-R132H (Table 2). Unfortunately, most derivatives containing substituents on the phenolic OH of C3, C6 and C7 position showed little or no activity. In addition, both **4** (β-mangostin) and **5** exhibited a much weaker and **8** (γ-mangostin) possessed a comparable but a little less potent inhibitory effects on IDH1-R132H, compared with **1** (Table 2). Together, our studies show that α-mangostin (**1**) represents the most potent core structure for the inhibition of IDH1-R132H.

Previous studies have demonstrated that a high level of *R*-2HG formed by heterozygous IDH1 mutations competitively inhibits a number of cellular α-KG-dependent dioxygenases, including histone lysine demethylases (KDMs) and the TET (ten-eleven translocation) family of DNA hydroxylases.[11] Histone KDMs remove the methyl group from the lysine residues of histone H3 and TETs catalyze a serial oxidative demethylation of 5-methylcytosine (5mC) into 5-hydroxymethylcytosine (5hmC), 5-formylcytosine (5fC) and 5-carboxylcytosine (5caC).[12] Therefore, we asked whether α-mangostin could promote demethylation of histone H3 trimethylated lysines and 5mC in IDH1-mutated cells. To address this issue, commercially-available isogenic IDH1 (+/+) and IDH1 (+/R132H) MCF10A cells, created by CRISPR/Cas9 technology (Horizon Discovery, Cambridge, United Kingdom) were purchased and exposed to α-mangostin for 24 h. As a result, we observed that α-mangostin did not affect the growth of both IDH1 (+/+) and IDH1 (+/R132H) MCF10A cells (Fig. 2A),[13] suggesting that α-mangostin is not cytotoxic to IDH1 (+/+) and IDH1 (+/R132H) MCF10A cells at this concentration. On the other hand, Western blot results show that IDH1 (+/R132H) MCF10A cells exhibited higher levels of histone H3 trimethylation at Lys4 (H3K4me3), Lys9 (H3K9me3), Lys27

Table 1
List of natural compounds used in our study and their effects on recombinant IDH1 and IDH1-R132H proteins

No.	Compound	Source	IDH1 activity (%)	IDH1-R132H activity (%)	No.	Compound	Source	IDH1 activity (%)	IDH1-R132H activity (%)
1	Daizin	ChromaDex	101.2 ± 2.86	94.7 ± 0.42	31	Ursolic acid	*Bridelia cambodiana*	102.2 ± 4.58	113.9 ± 8.50
2	Galangin	ChromaDex	89.1 ± 5.14	95.0 ± 1.95	32	Oleanolic acid	*Bridelia cambodiana*	100.9 ± 2.09	117.1 ± 3.82
3	Myricetin	ChromaDex	95.5 ± 6.16	93.2 ± 3.47	33	Stigmasterol	*Bridelia cambodiana*	111.3 ± 2.21	101.0 ± 5.04
4	Scutellarein	*Scutellaria baicalensis*	89.0 ± 0.73	92.0 ± 2.27	34	β-Sitosterol	*Bridelia cambodiana*	104.9 ± 1.14	98.8 ± 6.50
5	Chrysin	ChromaDex	97.6 ± 7.67	96.7 ± 1.52	35	Daucosterol	*Bridelia cambodiana*	105.4 ± 1.65	103.8 ± 5.53
6	Icaritin	ChromaDex	97.9 ± 4.48	94.6 ± 0.81	36	Gypenoside XVII	*Panax ginseng*	122.0 ± 3.74	101.9 ± 5.80
7	Scutellarin	*Scutellaria baicalensis*	88.8 ± 4.91	91.5 ± 3.49	37	Ginsenoside Rb1	*Panax ginseng*	116.7 ± 2.41	104.6 ± 5.87
8	Naringenin	ChromaDex	101.8 ± 1.67	109.3 ± 2.97	38	Imperatorin	*Saposhnikovia divaricata*	99.0 ± 2.49	101.8 ± 4.90
9	Populnetin	ChromaDex	103.6 ± 1.79	112.3 ± 2.50	39	Hamaudol	*Saposhnikovia divaricata*	98.2 ± 3.46	104.8 ± 5.65
10	Icariin	ChromaDex	90.4 ± 1.88	103.8 ± 1.28	40	3-*O*-Angeloylhamaudol	*Saposhnikovia divaricata*	97.8 ± 2.61	104.8 ± 4.08
11	Gartanin	*Garcinia mangostana*	89.9 ± 3.59	93.9 ± 7.22	41	5-*O*-Methylvisamminol	*Saposhnikovia divaricata*	102.8 ± 3.54	104.6 ± 3.88
12	8-Deoxygartanin	*Garcinia mangostana*	92.8 ± 1.65	108.8 ± 0.72	42	Ledebouriellol	*Saposhnikovia divaricata*	102.4 ± 1.45	108.4 ± 5.08
13	Isoliquiritigenin	*Glycyrrhiza glabra*	94.6 ± 6.27	98.1 ± 2.13	43	Gallic acid	ChromaDex	97.4 ± 3.70	103.1 ± 4.88
14	1-Isomangostin	*Garcinia mangostana*	100.0 ± 2.59	105.8 ± 2.53	44	Methoxyeugenol	*Cinnamomum cambodianum*	100.9 ± 1.91	103.6 ± 1.97
15	α-Mangostin	*Garcinia mangostana*	97.3 ± 3.44	43.2 ± 3.71	45	Spatulenol	*Thyrsanthera suborbicularis*	105.8 ± 1.81	107.2 ± 1.05
16	Lambertiainc acid	*Thuja orientalis*	100.2 ± 4.78	92.8 ± 1.57	46	Taraxerol	*Thyrsanthera suborbicularis*	106.0 ± 3.01	108.8 ± 1.10
17	Perviridamide	*Aglaia perviridis*	104.2 ± 5.81	95.9 ± 2.30	47	19-Hydroxy-1(10),15-rosadiene	*Thyrsanthera suborbicularis*	105.9 ± 1.71	115.9 ± 2.25
18	4-Hydroxy pyramidatine	*Aglaia perviridis*	100.3 ± 2.35	106.4 ± 3.55	48	Aleuritolic acid	*Thyrsanthera suborbicularis*	102.6 ± 0.61	113.3 ± 0.99
19	Pyramidatin	*Aglaia perviridis*	106.7 ± 0.59	100.0 ± 2.56	49	Marliolide	*Cinnamomum cambodianum*	110.8 ± 2.71	113.7 ± 1.58
20	Verproside	*Phseudolysimachion longifolium*	88.3 ± 4.09	107.1 ± 3.89	50	4′-*O*-β-D- Glucosyl-5-*O*-methylvisamminol	*Saposhnikovia divaricata*	107.1 ± 0.94	108.2 ± 1.94
21	Isovanillyl catalpol	*Phseudolysimachion longifolium*	102.5 ± 1.81	103.2 ± 1.48	51	Prim-*O*-glucosylcimifugin	*Saposhnikovia divaricata*	96.8 ± 5.93	111.8 ± 2.12
22	6-*O*-Veratroyl catalpol	*Phseudolysimachion longifolium*	107.1 ± 1.59	97.7 ± 0.98	52	1α,3β,6β-Trihydroxy-olean-12-ene (2)	*Vernicia fordii*	98.6 ± 5.47	99.0 ± 3.28
23	Minecoside	*Phseudolysimachion longifolium*	106.9 ± 1.27	107.7 ± 0.54	53	Castanopsol	*Vernicia fordii*	99.2 ± 1.24	110.7 ± 6.30
24	Diosmetin-7-*O*-Glc	*Phseudolysimachion longifolium*	107.5 ± 0.87	111.5 ± 1.06	54	Daturadiol	*Vernicia fordii*	102.1 ± 3.27	113.5 ± 0.36
25	Diosmetin-7-*O*-Glc-Xyl	*Phseudolysimachion longifolium*	103.9 ± 6.56	115.5 ± 0.39	55	2,3-Secofriedelan-2,3-oic acid	*Vernicia fordii*	107.9 ± 1.07	90.9 ± 1.02
26	3β-Friedelanol	*Bridelia cambodiana*	109.1 ± 0.14	112.8 ± 2.31	56	Cholesterol	*Vernicia fordii*	105.2 ± 2.53	96.3 ± 5.11
27	Friedelin	*Bridelia cambodiana*	103.8 ± 1.10	108.3 ± 1.12	57	Daucosterol	*Vernicia fordii*	94.6 ± 2.04	102.7 ± 7.49
28	24-Methyllanosta-9 (11),25-dien-3-one	*Bridelia cambodiana*	105.7 ± 0.76	123.9 ± 0.91	58	9-Hydroxycalabaxanthone	*Garcinia mangostana*	108.7 ± 0.86	98.7 ± 7.31
29	Betulinic acid	*Bridelia cambodiana*	101.5 ± 1.20	112.3 ± 2.02	59	Luteolin	ChromaDex	96.8 ± 5.24	93.6 ± 0.47
30	α-Amyrin	*Bridelia cambodiana*	105.3 ± 1.83	112.2 ± 1.02	60	Apigenin	ChromaDex	97.4 ± 1.67	84.0 ± 0.36

These chemicals were either directly purified from natural plants or purchased from the ChromaDex (Irvine, CA). Individual natural compounds were added to the reaction at 5 μM concentration and their effects were depicted as a percentage, compared to the control IDH1 and IDH1-R132H activities.

(H3K27me3), Lys36 (H3K36me3) and Lys79 (H3K79me3) compared with IDH1 (+/+) MCF10A cells, possibly due to a defect in the histone KDMs (Fig. 2B).[14] Likewise, our immunofluorescence results show that IDH1 (+/R132H) MCF10A cells exhibited a higher 5mC level (Fig. 2C, left panel), but lower 5hmC (Fig. 2C, middle panel) and 5fC (Fig. 2C, right panel) levels compared with IDH1 (+/+) MCF10A cells, presumably due to a defect in the activity of TET DNA hydroxylases.[15] Interestingly, treatment of α-mangostin selectively promoted a strong demethylation of histone H3 trimethylated lysines (H3K4me3, H3K9me3, H3K27me3, H3K36me3 and H3K79me3) in IDH1 (+/R132H) MCF10A cells (Fig. 2B). In addition, treatment of α-mangostin caused a selective decrease in the global 5mC level (Fig. 2C, left panel), but increased the global 5hmC (Fig. 2C, middle panel) and 5fC (Fig. 2C, right panel) levels in IDH1 (+/R132H) MCF10A cells. Together, these results imply that α-mangostin serves as a selective inhibitor of cellular IDH1-R132H.

A great deal of interests for development of selective IDH1-R132H chemical inhibitor(s) recently arose due to a high abundance and unique specificity of IDH1 mutations. Scientists from Agios Pharmaceuticals have reported the first selective chemical inhibitor of IDH1-R132H, for example, AGI-5198, which possesses

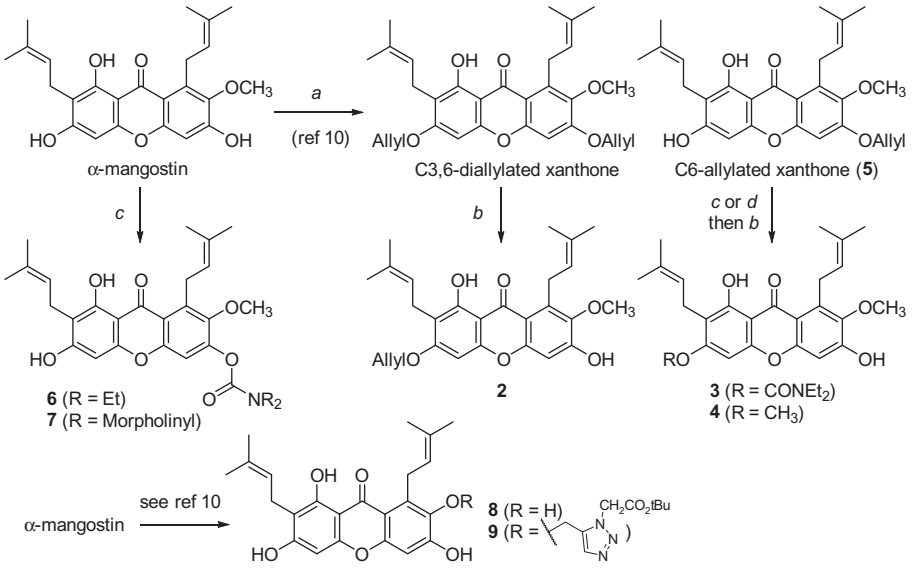

Scheme 1. Synthesis of α-mangostin derivatives. Reagents and conditions: (a) allyl bromide, K_2CO_3, acetone, 59% for **2**, 20% for **5**; (b) $Pd(PPh_3)_4$, K_2CO_3, MeOH, 60 °C, 91% for **4**; (c) diethylcarbamoyl chloride (for **3** and **6**), or morpholine-4-carbonyl chloride (for **7**), Et_3N, CH_2Cl_2; (d) MeI, K_2CO_3, acetone, 70%.

Table 2
The effect of α-mangostin derivatives on the IDH1-R132H activity

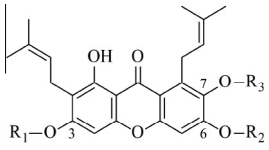

Compound	R_1	R_2	R_3	NADPH (μM)	Varied substrate	K_i (μM)
1 (α-mangostin)	–H	–H	$-CH_3$	150	α-KG	2.85 ± 0.2981
2		–H	$-CH_3$	150	α-KG	None
3	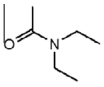	–H	$-CH_3$	150	α-KG	None
4 (β-mangostin)	$-CH_3$	–H	$-CH_3$	150	α-KG	12.0 ± 0.4815
5	–H		$-CH_3$	150	α-KG	17.4 ± 0.4268
6	–H	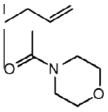	$-CH_3$	150	α-KG	None
7	–H	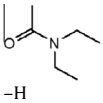	$-CH_3$	150	α-KG	None
8 (γ-mangostin)	–H	–H	–H	150	α-KG	3.17 ± 0.1681
9	–H	–H	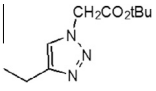	150	α-KG	None

The K_i value of α-mangostin against IDH1-R132H was acquired by the steady-state kinetic analysis.

the phenyl-glycine scaffold as a pharmacophore[16] and demonstrated that it selectively inhibited the growth of tumor cells, bearing a heterozygous IDH1-R132H in vivo.[17] Thereafter, development of additional selective IDH1-R132H inhibitors were accompanied. Davis et al. identified a novel stereo-selective inhibitor of IDH1-R132H, termed as (+)-ML309.[18] Liu et al. have reported a series of 1-hydroxypyridin-2-one compounds as new selective inhibitors of IDH1-R132H and IDH1-R132C.[19] Most recently, Deng et al. have identified a selective inhibitor of IDH1-R132H, bearing the bis-imidazole phenol structure.[20] In line with these findings, we have identified that α-mangostin is a new competitive inhibitor of IDH1-R132H. To the best of our knowledge, α-mangostin is the first natural compound that seems to selectively inhibit IDH1-R132H. In addition, we note that α-mangostin does not bear a structural resemblance with previous IDH1-R132H selective inhibitors.

General methods and materials: All starting materials and reagents were obtained from commercial suppliers and were used

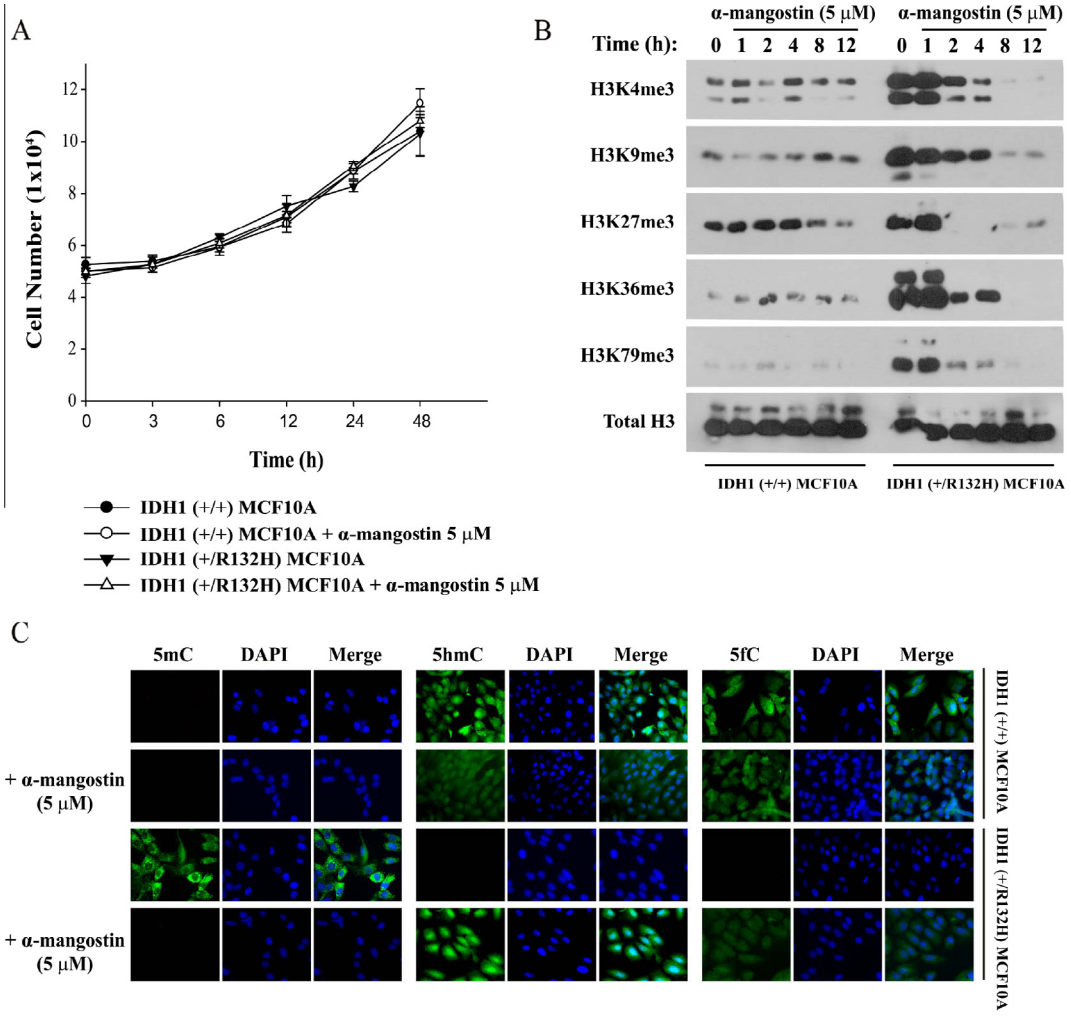

Figure 2. Selective demethylation of histone H3 trimethylated lysines and 5-methylcytosine is promoted by α-mangostin in IDH1 (+/R132H) MCF10A cells. (A) The overall cell viability of IDH1 (+/+) and (+/R132H) MCF10A cells is not affect by α-mangostin. (B) Western blot analysis indicates that α-mangostin selectively decreased the histone H3 trimethylated lysine levels in IDH1 (+/R132H) MCF10A cells. (C) α-mangostin selectively decreased the 5mC (left panel), but increased the 5hmC (middle panel) and 5fC (right panel) levels in IDH1 (+/R132H) MCF10A cells. The cell nucleus is visualized by DAPI staining and overlapped with individual fluorescent images.

without further purification. Air and moisture sensitive reactions were performed under an argon atmosphere. Flash column chromatography was performed using silica gel 60 (230–400 mesh, Merck) with the indicated solvents. Thin-layer chromatography was performed using 0.25 mm silica gel plates (Merck). ^{1}H and ^{13}C NMR spectra were recorded on either a Bruker 600 MHz, Bruker 500 MHz, or a JEOL 400 MHz spectrometer as solutions in deuteriochloroform ($CDCl_3$) or methanol-d4. ^{1}H NMR data were reported in the order of chemical shift, multiplicity (s, singlet; d, doublet; t, triplet; m, multiplet and/or multiple resonances), number of protons, and coupling constant (*J*) in hertz (Hz). Low resolution mass spectra were obtained on an Waters LCMS system (Waters 2489 UV/Visible Detector, Waters 3100 Mass, Waters 515 HPLC pump, SunFire C18 column 4.6 × 50 mm, 5 μm particle size, Waters 2545 Binary Gradient Module, Waters Reagent Manager, and Waters 2767 Sample Manager) with electrospray ionization. The compounds **4**, **5**, **8**, and **9** were prepared as our previous report.[10]

Experimental procedures and spectroscopic data: 3-(Allyloxy)-1,6-dihydroxy-7-methoxy-2,8-bis(3-methylbut-2-enyl)-9*H*-xanthen-9-one (**2**)

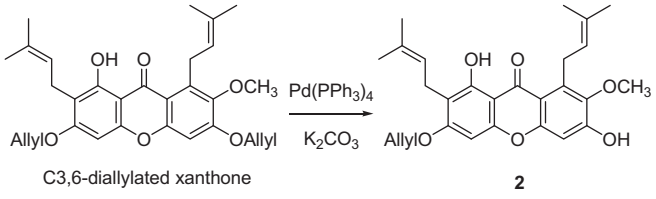

To a MeOH solution (5 mL) of diallylate xanthone (250 mg, 0.51 mmol), K_2CO_3 (140 mg, 1.01 mmol) and tetrakis(triphenylphosphine)palladium(0) (5 mg, 5 μmol) were added at ambient temperature. After stirring at 60 °C for 3 h, the reaction mixture was concentrated in vacuo. The residue was purified by flash column chromatography on silica gel (EtOAc/*n*-hexane = 1:2) to afford **2** (45 mg, 20%) as yellow solid. ^{1}H NMR (600 MHz, $CDCl_3$) δ 13.4 (s, 1H), 6.81 (s, 1H), 6.30 (s, 1H), 6.65 (s, 1H), 6.08–6.02 (m, 1H), 5.44 (dd, 1H, J = 1.8, 17 Hz), 5.31–5.28 (m, 1H), 5.26–5.23 (m, 2H), 4.61 (dt, 2H, J = 1.8 and 4.8 Hz), 4.10 (d, 2H, J = 6.0 Hz), 3.79 (s, 3H), 3.37 (d, 2H, J = 6.6 Hz), 1.83 (s, 3H), 1.80 (s, 3H), 1.69 (s, 3H), 1.68 (s, 3H); ^{13}C NMR (150 MHz, $CDCl_3$) δ 182.0, 162.3, 159.9,

155.6, 155.0, 154.6, 142.6, 137.1, 132.4, 132.0, 131.6, 123.2, 122.3, 117.7, 112.3, 111.7, 103.9, 101.5, 89.7, 69.1, 62.0, 31.6, 26.5, 25.8, 22.6, 21.5, 18.2, 17.9.

3,8-Dihydroxy-2-methoxy-1,7-bis(3-methylbut-2-enyl)-9-oxo-9*H*-xanthen-6-yl diethylcarbamate (**3**)

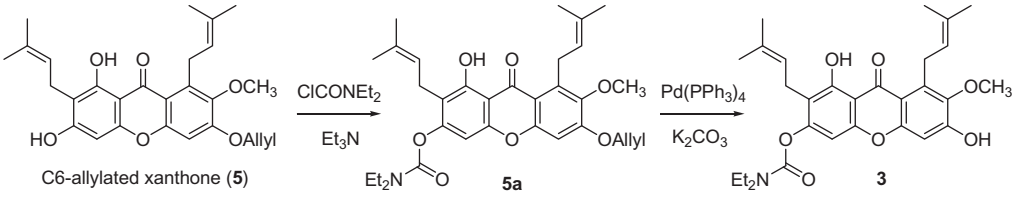

To a THF solution (5 mL) of **5** (16 mg, 0.037 mmol), sodium hydride (5 mg, 60%, 0.013 mmol) was added at 0 °C. After stirring for 30 min, diethylcarbamic chloride (5 mg, 0.037 mmol) was added. After stirring for 5 h at ambient temperature, the reaction mixture was extracted with EtOAc. A combined organic layer was washed with brine, dried over $MgSO_4$ and concentrated in vacuo. The residue was purified by flash column chromatography on silica gel (EtOAc/*n*-hexane = 1:3) to afford the **5a** (15 mg, 74%) as yellow solid. ^{1}H NMR (600 MHz, $CDCl_3$) δ 13.6 (s, 1H), 6.73 (s, 1H), 6.69 (s, 1H), 6.13–6.07 (m, 1H), 5.51 (dd, 1H, J = 1.2 and 17 Hz), 5.38 (dd, 1H, J = 1.2 and 11 Hz), 5.23 (t, 1H, J = 6.6 Hz), 5.17 (t, 1H, J = 6.6 Hz), 4.68 (d, 2H, J = 4.8 Hz), 4.13 (d, 2H, J = 6.6 Hz), 3.82 (s, 3H), 3.49–3.45 (m, 2H), 3.42–3.39 (m, 2H), 3.35 (d, 2H, J = 6.6 Hz), 1.85 (s, 3H), 1.76 (s, 3H), 1.68 (s, 3H), 1.67 (s, 3H), 1.28–1.23 (m, 6H); To a MeOH solution (5 mL) of **5a** (8 mg, 0.016 mmol), K_2CO_3 (10 mg, 0.072 mmol) and tetrakis(triphenylphosphine) palladium(0) (10 mg, 0.009 mmol) were added at ambient temperature. After stirring at 60 °C for 3 h, the reaction mixture was concentrated in vacuo. The residue was purified by flash column chromatography on silica gel (EtOAc/*n*-hexane = 1:2) to afford the **3** (4 mg, 57%) as yellow solid. ^{1}H NMR ($CDCl_3$, 600 MHz) δ 13.64 (s, 1H), 7.19 (s, 1H), 6.27 (s, 1H), 5.30 (m, 1H), 5.22 (m, 2H), 3.77 (s, 3H), 3.52–3.50 (m, 4H), 3.46–3.42 (m, 4H), 1.84 (s, 3H), 1.83 (s, 3H), 1.77 (s, 3H), 1.68 (s, 3H), 1.33–1.22 (m, 6H).

1,3-Dihydroxy-7-methoxy-2,8-bis(3-methylbut-2-enyl)-9-oxo-9*H*-xanthen-6-yl diethylcarbamate (**6**)

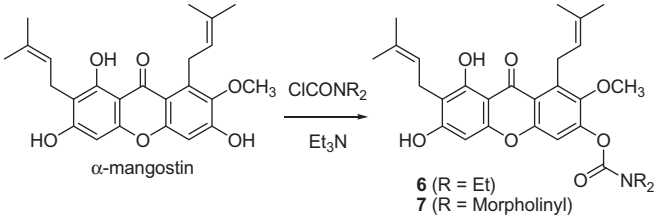

To a dichloromethane (5 mL) solution of α-mangostin (200 mg, 0.5 mmol), triethylamine (0.2 mL, 1.5 mmol) and diethylcarbamoyl chloride (135 mg, 1.0 mmol) were added at 0 °C. After stirring for 2 h at ambient temperature, the reaction mixture was extracted with EtOAc. A combined organic layer was washed with brine, dried over $MgSO_4$ and concentrated in vacuo. The residue was purified by flash column chromatography on silica gel (EtOAc/*n*-hexane = 1:4 to 1:2) to afford the carbamate **6** (65 mg, 26%) as yellow solid along with the bis-carbamate (56 mg, 18%). For **6**, ^{1}H NMR ($CDCl_3$, 400 MHz) δ 13.22 (s, 1H), 7.59 (s, 1H), 7.04 (s, 1H), 5.86 (s, 1H), 5.17 (m, 2H), 4.03 (d, 2H, J = 6.3 Hz), 3.73 (s, 3H), 3.53–3.44 (m, 4H), 3.29 (d, 2H, J = 6.8 Hz), 1.80–1.63 (m, 12H), 1.33–1.22 (m, 6H). For bis-carbamate, ^{1}H NMR ($CDCl_3$, 400 MHz) δ 13.34 (s, 1H), 7.18 (s, 1H), 6.69 (s, 1H), 5.19 (m, 2H), 4.12 (d, 2H, J = 6.3 Hz), 3.75 (s, 3H), 3.44–3.37 (m, 8H), 3.33 (d, 2H, J = 6.8 Hz), 1.81–1.65 (m, 12H), 1.24–1.20 (m, 12H); ^{13}C NMR ($CDCl_3$, 100 MHz) δ 182.9, 160.7, 155.7, 154.1, 153.8, 152.9, 152.6, 150.0, 146.8, 138.5, 132.0, 131.9, 122.9, 121.7, 116.1, 116.0, 110.6, 100.1, 61.6, 42.2, 42.0, 41.9, 26.4, 25.8, 25.6, 22.2, 18.1, 17.8, 14.2, 13.2.

1,3-Dihydroxy-7-methoxy-2,8-bis(3-methylbut-2-enyl)-9-oxo-9*H*-xanthen-6-yl morpholine-4-carboxylate (**7**)

To a dichloromethane (5 mL) solution of α-mangostin (200 mg, 0.5 mmol), triethylamine (0.2 mL, 1.5 mmol) and morpholinecarbonyl chloride (149 mg, 1.0 mmol) were added were added at 0 °C. After stirring for 5 h at ambient temperature, the reaction mixture was extracted with EtOAc. A combined organic layer was washed with brine, dried over $MgSO_4$ and concentrated in vacuo. The residue was purified by flash column chromatography on silica gel (EtOAc/*n*-hexane = 1:4) to afford the carbamate **7** as yellow solid along with a bis-carbamate. For **7**, ^{1}H NMR ($CDCl_3$, 400 MHz) δ 13.40 (s, 1H), 7.09 (s, 1H), 6.07 (s, 1H), 5.22–5.15 (m, 2H), 4.08 (d, 2H, J = 6.3 Hz), 3.79–3.73 (m, 13H), 3.38 (d, 2H, J = 7.3 Hz), 1.80 (s, 3H), 1.79 (s, 3H), 1.71 (s, 3H), 1.65 (s, 3H); ^{13}C NMR ($CDCl_3$, 100 MHz) δ 181.7, 161.9, 160.6, 154.6, 153.9, 152.6, 149.0, 146.6, 138.8, 134.5, 131.8, 123.1, 121.6, 116.6, 110.4, 109.1, 103.5, 93.1, 66.6, 66.5, 6.7, 45.1, 44.4, 26.3, 25.8, 21.4, 18.2, 17.8; For bis-carbamate, ^{1}H NMR ($CDCl_3$, 400 MHz) δ 13,41 (s, 1H), 7,18 (s, 1H), 6.69 (s, 1H), 5.17 (d, 2H), 4.12 (d, 2H, J = 6.3 Hz), 3.75–3.58 (m, 22H), 3.32 (d, 2H, J = 6.8 Hz), 1.81 (s, 3H), 1.74 (s, 3H), 1.66 (s, 3H), 1.53 (s, 3H); ^{13}C NMR ($CDCl_3$, 100 MHz) δ 182.8, 160.8, 155.3, 154.1, 153.7, 152.0, 149.7, 146.8, 138.8, 132.1, 122.7, 121.6, 116.2, 110.6, 100.2, 66.6, 66.5, 61.7, 44.4, 26.4, 25.8, 25.7, 22.2, 18.2, 17.8.

Acknowledgements

This research was supported by the Bio & Medical Technology Development Program of the National Research Foundation (NRF) funded by the Ministry of Science, ICT & Future Planning (No. 2012M3A9C1053532). We have competing financial interests related to this study.

References and notes

1. Warburg, O. *Science* **1956**, *123*, 309.
2. Tripathy, D.; Harnden, K.; Blackwell, K.; Robson, M. *BMC Med.* **2014**, *12*, 140.
3. Parsons, D. W.; Jones, S.; Zhang, X.; Lin, J. C.; Leary, R. J.; Angenendt, P.; Mankoo, P.; Carter, H.; Siu, I. M.; Gallia, G. L.; Olivi, A.; McLendon, R.; Rasheed, B. A.; Keir, S.; Nikolskaya, T.; Nikolsky, Y.; Busam, D. A.; Tekleab, H.; Diaz, L. A., Jr.; Hartigan, J.; Smith, D. R.; Strausberg, R. L.; Marie, S. K.; Shinjo, S. M.; Yan, H.; Riggins, G. J.; Bigner, D. D.; Karchin, R.; Papadopoulos, N.; Parmigiani, G.; Vogelstein, B.; Velculescu, V. E.; Kinzler, K. W. *Science* **2008**, *321*, 1807.
4. Losman, J. A.; Kaelin, W. G., Jr. *Genes Dev.* **2013**, *27*, 836.
5. Keum, Y. S.; Choi, B. Y. *BMB Rep.* **2015**, *48*, 266.
6. Dang, L.; White, D. W.; Gross, S.; Bennett, B. D.; Bittinger, M. A.; Driggers, E. M.; Fantin, V. R.; Jang, H. G.; Jin, S.; Keenan, M. C.; Marks, K. M.; Prins, R. M.; Ward,

P. S.; Yen, K. E.; Liau, L. M.; Rabinowitz, J. D.; Cantley, L. C.; Thompson, C. B.; Vander Heiden, M. G.; Su, S. M. *Nature* **2009**, *462*, 739.

7. Human IDH1 cDNA (GenBank Number, AF020038) was purchased from Korea Human Gene Bank (Daejeon, Republic of Korea). A site-directed mutagenesis using an overlapping PCR was conducted to create a mutant IDH1 (IDH1-R132H) cDNA. Both wild-type and mutant IDH1 cDNAs were subcloned into the pET21 vector and transformed into BL21 cells. Cells were grown in LB media at 37 °C until OD600 reaches at the absorbance of 0.6. Recombinant proteins were induced by adding isopropyl-β-D-thiogalacto-pyranoside (IPTG) with a final concentration of 1 mM for 4 h. Cell were resuspended in cell lysis buffer (20 mM Tris–Cl, pH 7.4, 0.1% (v/v) Triton X-100, 500 mM NaCl, 1 mM PMSF, 5 mM β-mercaptoethanol, 10% (v/v) glycerol) and heavily sonicated in 4 times for every 30 s. Samples were centrifuged at 12,000 rpm for 1 h and supernatant was loaded in Ni^{2+}-affinity resin (GE Healthcare, Piscataway, NJ), which was previously activated with buffer 1 (20 mM Tris–Cl, pH 7.4, 500 mM NaCl, 5 mM β-mercaptoethanol, 10% (v/v) glycerol). Resin was washed by buffer 1 three times and the sample elution was performed with an appropriate volume of buffer 2 (20 mM Tris–Cl, pH 7.4, 500 mM NaCl, 5 mM β-mercaptoethanol, 500 mM imidazole, 10% (v/v) glycerol). Eluted samples were dialyzed twice with buffer 3 (50 mM Tris–Cl, pH 7.4, 200 mM NaCl, 5 mM β-mercaptoethanol, 2 mM MnSO4, 10% (v/v) glycerol) and stored at −80 °C for future biochemical analyses.
8. The IDH activity was assayed by measuring the reduction of $NADP^+$ into NADPH or the oxidation of NADPH into $NADP^+$ with spectrophotometry, based on the principle that NADPH, but not $NADP^+$, possesses an optical absorption at 340 nm. In order to measure the reduction of $NADP^+$ into NADPH, 0.5 μg recombinant protein was added to 200 μL assay solution (100 mM Tris–Cl, pH 7.5, 1.3 mM MnCl2, 0.33 mM EDTA, 0.5 mM β-NADP + 0.5 mM D(+)-threo-isocitrate) and the resulting absorbance was measured at 340 nm after 5 min. In order to measure the oxidation of NADPH into $NADP^+$, 5 μg recombinant protein added to 200 μL assay solution (100 mM Tris–Cl, pH 7.5, 1.3 mM $MnCl_2$, 0.5 mM β-NADPH, 2.5 mM α-ketoglutarate) and the decreasing absorbance was measured at 340 nm after 5 min. The measurement of NADPH levels was conducted, using the spectraMax M3 spectrophotometer (Molecular Devices, Sunnyvale, CA).
9. A sufficient amount of IDH1-R132H was added to the reaction solution (150 mM NaCl, 20 mM Tris–Cl, pH 7.5, 10 mM $MnCl_2$, 150 μM β-NADPH, 0.03% (w/v) bovine serum albumin) and various concentrations of α-ketoglutarate were added to monitor the maximal enzyme activity. The acquisition of steady-state kinetic parameters were conducted using the enzyme kinetics module, equipped in Sigmaplot software (Systat Software, San Jose, CA).

10. Fei, X.; Jo, M.; Lee, B.; Han, S.-B.; Lee, K.; Jung, J.-K.; Seo, S.-Y.; Kwak, Y.-S. *Bioorg. Med. Chem. Lett.* **2014**, *24*, 2062.
11. Cairns, R. A.; Mak, T. W. *Cancer Discov.* **2013**, *3*, 730.
12. Oermann, E. K.; Wu, J.; Guan, K. L.; Xiong, Y. *Semin. Cell Dev. Biol.* **2012**, *23*, 370.

13. IDH1 (+/+) and IDH1 (+/R132H) MCF10A cells were grown in DMEM/F-12 media (Welgene, Deagu, Republic of Korea), supplemented with 5% horse serum (Welgene, Deagu, Republic of Korea), 20 ng/mL EGF, 0.5 μg/mL hydrocortisone, 10 μg/mL insulin. IDH1 (+/+) and IDH1 (+/R132H) MCF10A cells were seeded in 6 well plates at the number of 5.0×10^4 per well. After an exposure to 5 μM α-mangostin. cells were collected after indicated times and the viable cell number was calculated, using hemacytometer counting. Data are shown in mean ± standard deviation and a statistical analysis was conducted with Student *t*-test ($n = 6$).
14. % confluent MCF10A cells were exposed to 5 μM α-mangostin and cell lysates were collected with 200 μL SDS lysis buffer [50 mM Tris–HCl at pH 8.0, 150 mM NaCl, 1% NP-40, 0.5% deoxycholic acid, 1% sodium dodecyl sulfate (SDS), 1 mM Na_3VO_4, 1 mM dithiothreitol (DTT), 1 mM phenylmethylsulfonyl fluoride (PMSF)] and kept on ice for 30 min. After centrifugation at 12,000 rpm for 10 min, protein concentration was measured using a BCA Protein Assay Kit (Thermo Fisher Scientific, Waltham, MA). Cell lysates were resolved by SDS-PAGE and transferred to PVDF membranes (BioRad, Hercules, CA). The membranes were incubated in blocking buffer (5% skim milk in 1× PBS-0.1% Tween-20, PBST) for 1 h and further hybridized with the appropriate primary antibodies in 1× PBS containing 3% bovine serum albumin (BSA) or 3% skim milk overnight at 4 °C. Primary antibodies used in our study are as follows: H3K4me3 (Millipore, 04-745), H3K9me3 (Abcam, ab8898), H3K27me3 (Millipore, 07-449), H3K36me3 (Abcam, ab9050), H3K79me3 (Abcam, ab2621) and total H3 (Millipore, 05-928). After washing three times with 1× PBST for 30 min, the membrane was hybridized with horseradish peroxidase (HRP)-conjugated secondary antibody (Santa Cruz Biotechnology, Santa Cruz, CA) for 1 h at room temperature and washed three times with 1× PBST solution for 30 min. The membrane was visualized by using an enhanced chemiluminescence (ECL) detection.
15. IDH1 (+/+) and IDH1 (+/R132H) MCF10A cells were seeded in 24 well plates (5×10^4 cells per well in cover glass) and incubated at 37 °C for 16 h and exposed to 5 μM α-mangostin for additional 24 h. After fixation with 4% paraformaldehyde for 15 min, cells were incubated with blocking buffer (1% horse serum, 0.1% triton X-100 in PBS) for 1 h and hybridized against 5mC (Active Motif, 39649), 5hmC (Active Motif, 39769), 5fC (Active Motif, 61223) antibodies overnight. After washing three times with 1x PBS for 30 min, cells were incubated FITC-conjugated secondary antibody solutions, containing DAPI at room temperature for 1 h and washed three times with 1x PBS solution for 30 min. Samples on a slide glass were immersed in mounting medium and the fluorescence image was captured on Eclipse Ti fluorescence microscopy, equipped with NIS Elements software (Nikon, Tokyo, Japan).

16. Popovici-Muller, J.; Saunders, J. O.; Salituro, F. G.; Travins, J. M.; Yan, S.; Zhao, F.; Gross, S.; Dang, L.; Yen, K. E.; Yang, H.; Straley, K. S.; Jin, S.; Kunii, K.; Fantin, V. R.; Zhang, S.; Pan, Q.; Shi, D.; Biller, S. A.; Su, S. M. *ACS Med. Chem. Lett.* **2012**, *3*, 850.
17. Rohle, D.; Popovici-Muller, J.; Palaskas, N.; Turcan, S.; Grommes, C.; Campos, C.; Tsoi, J.; Clark, O.; Oldrini, B.; Komisopoulou, E.; Kunii, K.; Pedraza, A.; Schalm, S.; Silverman, L.; Miller, A.; Wang, F.; Yang, H.; Chen, Y.; Kernytsky, A.; Rosenblum, M. K.; Liu, W.; Biller, S. A.; Su, S. M.; Brennan, C. W.; Chan, T. A.; Graeber, T. G.; Yen, K. E.; Mellinghoff, I. K. *Science* **2013**, *340*, 626.
18. Davis, M. I.; Gross, S.; Shen, M.; Straley, K. S.; Pragani, R.; Lea, W. A.; Popovici-Muller, J.; DeLaBarre, B.; Artin, E.; Thorne, N.; Auld, D. S.; Li, Z.; Dang, L.; Boxer, M. B.; Simeonov, A. *J. Biol. Chem.* **2014**, *289*, 13717.
19. Liu, Z.; Yao, Y.; Kogiso, M.; Zheng, B.; Deng, L.; Qiu, J. J.; Dong, S.; Lv, H.; Gallo, J. M.; Li, X. N.; Song, Y. *J. Med. Chem.* **2014**, *57*, 8307.
20. Deng, G.; Shen, J.; Yin, M.; McManus, J.; Mathieu, M.; Gee, P.; He, T.; Shi, C.; Bedel, O.; McLean, L. R.; Le-Strat, F.; Zhang, Y.; Marquette, J. P.; Gao, Q.; Zhang, B.; Rak, A.; Hoffmann, D.; Rooney, E.; Vassort, A.; Englaro, W.; Li, Y.; Patel, V.; Adrian, F.; Gross, S.; Wiederschain, D.; Cheng, H.; Licht, S. *J. Biol. Chem.* **2015**, *290*, 762.